Journal of. Modern Trends in Physics Research
Online ISSN 2636-4220
DOI: 10.19138/mtpr/(14)137-147
Accepted: 2014-12-19

Interactions in nuclear emulsion detector irradiated by α–particle

A. Abdelsalam[1], Z. Abou–moussa[1], W. Osman[1], B. M. Badawy[2,*], H. A. Amer[2], M. M. El–Ashmawy[3], N. Abdallah[3]

[1] *Physics Department, Faculty of Science, Cairo University, Giza, Egypt.*
[2] *Reactor Physics Department, Nuclear Research Center, Atomic Energy Authority, Egypt.*
[3] *Nuclear and Radiological Regulatory Authority, NRRA, Egypt.*

[*] ***Corresponding author*** - he_cairo@yahoo.com

Abstract- Using the multiplicity characteristics of the final state hadron, the shower particles emitted in the 4–pspace through 4He interactions with emulsion nuclei are studied in a few A GeV region. Basing on a universality of state, the multiplicity distributions, in the backward hemisphere of the space, are determined as a function of the target size. The shower particle multiplicity, while found to depend only on the target size in the backward hemisphere, depends on both the energy and system size in the forward hemisphere. It is seen that the shower particles are originated from two emission sources. One of both emits pion in the backward hemisphere, beyond the kinematic limits, as a target source particle regarding the limiting fragmentation hypothesis. The other is the main source which emits pion in the forward hemisphere as a result of a particle creation system. The results are analyzed in the framework of the Lund Monte–Carlo program code–events generating FRITIOF model.

Keywords- Dubna Energies; Shower Particle Sources; Target Size Dependence; FRITIOF Model.

1. INTRODUCTION

At low energy the physics can be accounted for fairly well by one single source. The de–excitation can be understood in terms of particle emission from a liquid drop of nuclear matter. At high energy, multiple sources are needed. The de–excitation is here understood in terms of particle emission from an expanding gas of nuclear matter in thermodynamical equilibrium. At excitation energies comparable with the total binding energy, ~ 5A to 8A MeV, the very existence of a long–lived compound nucleus becomes unlikely. In this situation an explosion–like process leads to the total disintegration of the nucleus and the multiple emission of nuclear fragments of different masses (1 and references therein). One can come to the multifragmentation concept from a quite different starting point, by considering a liquid–gas phase transition in excited nuclear matter. The name "multifragmentation" is introduced firstly in Ref. (2). At high energy collisions, the produced particles are not confined up to nuclear fragments, but they include essentially created particles the so called hadrons.

It is known that, the radiation therapy is the medical use of ionizing radiation to treat cancer. In conventional radiation therapy, beams of X–rays (high energy photons) are produced by accelerated electrons and then delivered to the patient to destroy tumor cells. Using crossing beams from many angles, radiation oncologists irradiate the tumor target while trying to spare the surrounding normal tissues. Inevitably some radiation dose is always deposited in the healthy tissues. Initially, the clinical applications are limited to few parts of the body since the accelerators are not powerful enough to allow protons to penetrate deep in the tissues. The improvements in accelerator technology coupled with advances in medical imaging and computing, make proton therapy a viable option for routine medical applications. Therefore, proton becomes the most common type of particle therapy. However, the photon as a particle is used in X–ray and γ–ray, the so called photon therapy. Muon and electron, the so called lepton therapy, are occasionally attempted. All the particles that are constructed of quarks (hadrons) are not elementary. Therefore, in their usage, it is more correctly to say hadron therapy. When the irradiating beams are made of charged particles (protons, α–particle, and heavier ions), radiation therapy is also called hadron therapy or heavy–ion therapy. The strength of hadron therapy lies in the unique physical and radiobiological properties of these particles. They can penetrate the tissues with little diffusion and deposit the maximum energy just before stopping. This allows a precise definition of the specific region to be irradiated. With the use of the hadron the tumor can be irradiated while the

Journal of. Modern Trends in Physics Research
Online ISSN 2636-4220
DOI: 10.19138/mtpr/(14)137-147
Accepted: 2014-12-19

damage to healthy tissues is less than with X–rays. Although protons are used in several hospitals, the next step in radiation therapy is the use of carbon ions. These have some clear advantages even over protons in providing both a local control of very aggressive tumors and a lower acute or late toxicity. At HIMAC (NIRS, Chiba, Japan) Kanai et al Ref. (3 and references therein) study the fragmentation of (0.09A and 0.5A GeV iron) and 0.4A GeV krypton beams in tissue equivalent material. For radiotherapy at GSI (Darmstadt, Germany) information on carbon fragmentation in tissue–like materials is of great interest [4, 5]. For shielding applications, relatively light ions such as helium, carbon, neon, and silicon are worth studying both in their own right and because they are produced as secondary fragments by interactions of heavier primary ions in shielding and in the human body. In support of the HIMAC radiotherapy program, Kanai et al Ref. (3 and references therein) use the fragmentation of (0.15A GeV, 0.29A, and 0.4A GeV) ^{12}C, 0.4A GeV ^{20}Ne, 0.49A GeV ^{28}Si, and 0.55A GeV ^{40}Ar on C5H8O2 target.Malakhov et al Ref. (3 and references therein) measure fragments produced by a 1.044A GeV d beam in a gold target at the Nuclotron of Dubna, Russia. Although these measurements are with a heavy target, the number of light ions produced in secondary collisions makes them relevant, and argues for further measurements, perhaps with shielding and tissue equivalent targets. At Lawrence Berkeley National Laboratory, LBNL, of USA Miller present measurements for hadron therapy over energy range of 0.1A up to 1A GeV [3]. At the end of 2008, about 28 treatment facilities are in operation worldwide and over 70,000 patients can be treated by means of pions[6–8], protons, and heavier ions. In Europe, the interest in hadron therapy grows rapidly and the first heavy–ion clinical facility in Heidelberg, Germany, starts treating patients at the end of 2009[9]. While the advantages of protons over photons are quantitative in terms of the amount and distribution of the delivered dose, several studies show evidence that carbon ions damage cancer cells in a way that the cells can not repair themselves. Carbon therapy may be the optimal choice to tackle radio–resistant tumors; other light ions, such as helium, are also being investigated [10].

On the other hand, the high–energy hadron–hadron, hadron–nucleus, or nucleus–nucleus interactions are a precise source in which all categories of secondary emitted particles are available. It is very important to learn as much as possible about all the phenomena which occur in this interactions to observe the anticipated signatures on the background of "normal phenomena". Some of these phenomena are the hadron production, projectile fragmentation, target fragmentation, the multiplicity and emission characteristics, the reaction cross sectional behavior, and the stopping power of the target materials in the voted detector with respect to each passing particle. Hence, the choice of projectiles, targets, energies, and the critical parameters in measurements motivates the correct modeling and simulation of the therapy planning. Actually, the synchrophasotron accelerator at Dubna enables equipping beams of $A \geq 1$, in a few A GeV range of energies. This region is a special energy, at which the nuclear limiting fragmentation applies initially[11–17]. The nuclear emulsion is a very useful tool in experimental physics for investigating atomic and nuclear processes. It can be used as a detector of 4–πspace geometry. It contains target materials over a wide range of mass numbers, ^{1}H, ^{12}C, ^{14}N, ^{16}O, ^{82}Br, ^{108}Ag. It has the possibility of measuring energies and angles with high degree of resolution. It can be used in studying the characteristics of new elementary particles and can detect the decay of the unstable neutral particles, rather than, its sensitivity to slow charged particles arising from the disintegration of the target nucleus. Owing to the high stopping power of emulsion, a large fraction of short–lived particles is brought to rest in it before decay and hence their ranges and life times can be measured accurately. In this work the interactions of α–particle with emulsion nuclei are study at Dubna energies (2.1A and 3.7A GeV). The investigation of relativistic hadron (shower particle) production, according to the emission angular zone and target size effect, is focused.

EXPERIMENTAL DETAILS

The NIKFI–BR2 nuclear emulsion stacks used this experiment are irradiated by α–particle beams at the Synchrophasotron of JINR in Dubna, Russia. The beams energies are 2.1A and 3.7A GeV. Each emulsion pellicle size is 20 cm × 10 cm × 0.06 cm. Table (1) shows the chemical composition of this emulsion type.

Table (1): The chemical composition of NIKFI–BR2 emulsion.

Element	^{1}H	^{12}C	^{14}N	^{16}O	^{80}Br	^{108}Ag
Atoms /cm^3×1022	3.150	1.410	0.395	0.956	1.028	1.028

The obeyed methods, equipment, and experimental restrictions are as similar as detailed in experiments[18, 19].

Journal of. Modern Trends in Physics Research
Online ISSN 2636-4220
DOI: 10.19138/mtpr/(14)137-147
Accepted: 2014-12-19

The produced particles are identified in photographic nuclear emulsion, according to the commonly accepted ionization behavior[20, 21], as:

- Shower particles having $g \leq 1.4g_p$ where g is the track grain density and g_p corresponds to the grain density of the minimum ionizing track. These particles are relativistic hadrons, which consist mainly of pions and less than 10% mesons and baryons. Their multiplicity is denoted as ns. The notations n_s^f and nsb are corresponding to the shower particles emitted in the FHS and BHS, respectively.
- Grey particles having a range > 3 mm and $1.4g_p < g \leq 4.5g_p$; they are mainly recoil protons knocked–out from the target nucleus during the collision. Their kinetic energy ranges from 26 up to 400 MeV.
- Black particles having a range ≤ 3 mm and $g > 4.5g_p$; they are evaporated target protons with kinetic energy < 26 MeV.
- The grey and black particles together amount the group of the target fragments, the so called heavily ionizing particles. These fragments are emitted in the 4–π space. Their multiplicity is denoted as N_h.
- The projectile fragments having $Z \geq 1$; they are fragmented nuclei having nearly the same momentum of the incident nucleus. They are emitted in a very narrow forward cone along the direction of incidence.

RESULTS and DISCUSSION

Interaction Cross–Section

Listed in Table (2) are the total scanned lengths, L, of the primary beam tracks; the number of resulting inelastic interactions, N; and the corresponding average values of the experimental mean free path, λ. The mean free path of α–particle in the NIKFI–BR2 emulsion type is predicted using a Glauber's approach simulation code[22] as, 18.79 cm. It is concluded from Table (2) that the mean free path of α–particle in nuclear emulsion is not sensitive to the energy where the measured and predicted values are nearly in agreement with each other.

Table (2): Beams interactions data.

E_{lab}/A GeV	L m	N Events	λcm
2.1	416.5	2066	20.16±0.44
3.7	217.6	1092	19.93±0.60

Since the nuclear emulsion is a homogeneous mixture of different nuclei, the inelastic interactions can be classified into groups according to the target nucleus. In this experiment the events discrimination is executed using the widely explained methods[19] & [23–27] and the theoretical predictions of the Glauber's approach[22]. The present inelastic interactions cross sections with H, CNO, and AgBr are correlated in Fig. (1) with the target size.

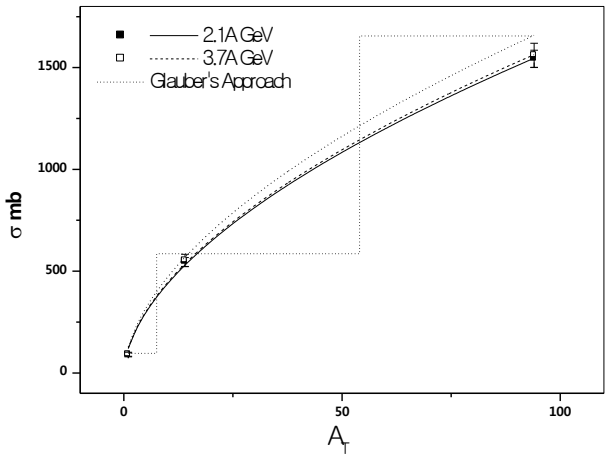

Journal of. Modern Trends in Physics Research
Online ISSN 2636-4220
DOI: 10.19138/mtpr/(14)137-147
Accepted: 2014-12-19

Fig. (1): The cross section of the present α–particle inelastic interactions in nuclear emulsion as a function of the target size, together with the predictions of the Glauber's approach (histogram).

From Fig. (1), the cross sectional values are nearly the same at the two used energies. The Glauber's approach can predict them well. The data are approximated by the power law relation of Eq. (1) which is presented by the smooth curves in Fig. (1). the fit parameters, α and β, are listed in Table (3). The fit parameters are α ~ 120 and β = 0.56 ~ 2/3. Therefore, Eq. (1) can be rewritten as Eq. (2).

$$\sigma = \alpha A_T^{\beta} \quad (1)$$

$$\sigma = 120 A_T^{0.56}\,\mathrm{mb} \quad (2)$$

Table (3): The fit parameters of Eq. (1).

Fit Parameter	α	β
E_{lab} = 2.1A GeV	119.74±16.43	0.56±0.03
E_{lab} = 3.7A GeV	121.46±17.10	0.56±0.03
Glauber's Approach Prediction	128.54±17.88	0.56±0.03

Multiplicity Distributions

In what follows, the inelastic interaction samples of 2.1A and 3.7A GeV α–particle in nuclear emulsion are separated into statistical groups according to the target sizes. Applying the predicted percentages of Glauber's theory encoded in Ref. (22), we categorize the data according to the interactions with H, CNO, Em, and AgBr targets separately. The effective mass number of each target group of nuclei is 1, 14, 70, and 94, respectively. The modified FRITIOF code is used to simulate the present data. It is based on the Lund version 1.6[27, 28]. The modification was carried out by V. V. Uzhinskii, LIT, JINR, Dubna, Russia, in 1995. The predictions of the model are presented in the enclosed figures by histograms and they are placed between round brackets throughout the tables.

In Fig. (2) the backward emitted shower particle multiplicity distributions associated with the present interactions are shown. For all targets, the characteristic feature of the distribution is the exponential decay shape. The multiplicity range (decay tail) exceeds with the target size. For α–particle, as a light projectile, the energy seems to have a qualitatively considerable effect. This effect is reflected on the longer distributions tails at 3.7A GeV than at 2.1A GeV. The characteristic exponential behavior can be approximated by Eq. (3). The fit parameters, P_s^b and λ_s^b, are listed in Table (4).

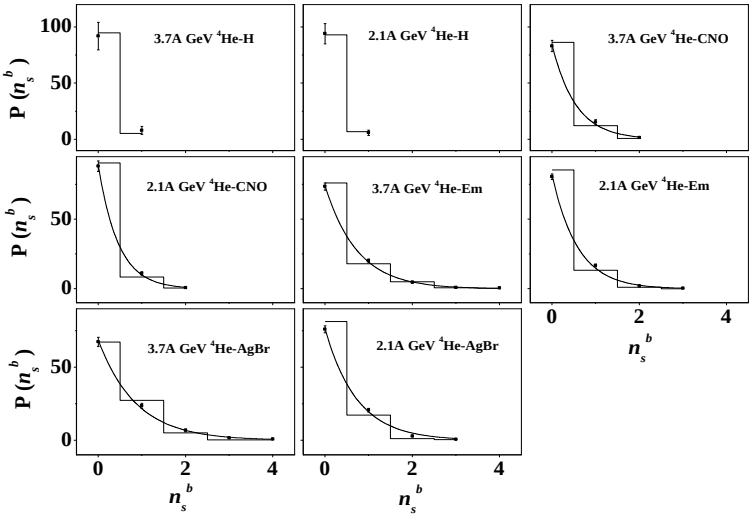

Journal of. Modern Trends in Physics Research
Online ISSN 2636-4220
DOI: 10.19138/mtpr/(14)137-147
Accepted: 2014-12-19

Fig. (2): The multiplicity distributions of the backward shower particle emitted in 2.1A and 3.7A GeV ^{4}He interactions with H, CNO, Em, and AgBr nuclei, together with the predictions of the modified FRITIOF model and the exponential decay fitting.

$$P(n_s^b) = p_s^b e^{-\lambda_s^b n_s^b} \quad (3)$$

The data are reproduced well by the model. The exponential fit of the experimental data and their theoretical predications are presented by the solid and dashed curves, respectively.In Table (4), the fit parameters are affected weakly by energy. The small energy effect consists of a longer decay tail of the distributions at 200A GeV than at 3.7A GeV. This effect is attributed to more excitation in the target nucleus at the higher energy. Consequently, the produced compound nucleus will de–excite and decay by emitting this excess number of backward hadrons. Such a mechanism of compound target nucleus was discussed in experiments[29, 30]. Therefore, regarding the nuclear limiting fragmentation beyond 1A GeV, the projectile energy cannot be considered an effective parameter in the backward production and consequently does not mean that, this system of particle production is a creation system. The values associated by the model in Table (4) often agree with the measured ones.

Table (4): The fit parameters of Eq. (3).

E_{lab}/A **GeV**	Target	λ_s^b	P_s^b
2.1	CNO	2.18±0.11 (2.36±0.02)	88.64±3.73 (90.43±0.15)
	Em	1.71±0.04 (1.87±0.05)	81.65±1.95 (85.42±0.69)
	AgBr	1.37±0.08 (1.60±0.09)	76.10±1.75 (81.29±1.61)
3.7	CNO	1.84±0.12 (1.97±0.06)	84.00±4.96 (86.48±0.71)
	Em	1.35±0.05 (1.43±0.03)	74.04±2.52 (76.17±0.51)
	AgBr	1.16±0.05 (1.05±0.11)	68.44±2.98 (67.90±3.28)

The backward emitted shower particle multiplicity at the two incident energies can be determined as a function of the effective target mass, A_T, as in Fig. (3). Therefore, the fit parameters of Table (4) are correlated with A_T. The linear fitting is approximated by Eq. (4) and Eq. (5) and presented by the straight lines. The solid and dashed lines belong to the correlation associated by the measured data and their theoretical predictions, respectively. The fit parameters of Eq. (4) and Eq. (5) are shown in Table (5). The slope and intercept parameters decrease linearly with the target mass. Therefore, the backward emission of the relativistic hadronstrongly depends on the target size.

$$\lambda_s^b = a_\lambda + b_\lambda A_T \quad (4)$$

$$P_s^b = a_p + b_p A_T \quad (5)$$

Journal of. Modern Trends in Physics Research
Online ISSN 2636-4220
DOI: 10.19138/mtpr/(14)137-147
Accepted: 2014-12-19

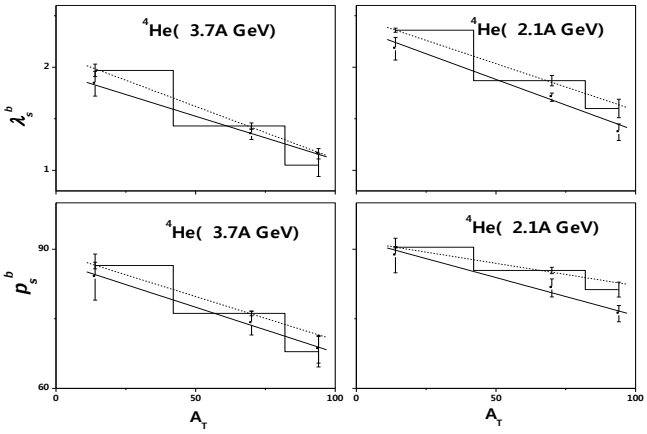

Fig. (3): The fit parameters of Eq. (3) as a function of the target size.

Table (5): The fit parameters of Eq. (4) and Eq. (5).

E_{lab}/A GeV	2.1	3.7
a_λ	2.38±0.15 (2.49±0)	1.95±0.02 (2.13±0.09)
b_λ	–0.01±0 (–0.0±0)	–0.01±0 (–0.0±0)
a_p	92.07±0.07 (91.78±0.25)	87.27±1.42 (89.18±1.02)
b_p	–0.16±0.04 (–0.10±0.01)	–0.20±0.02 (–0.19±0.02)

In Fig. (4) the forward emitted shower particle multiplicity distributions of the present interactions are shown. Unlike the observed behavior of the backward emitted shower particle, the characteristic feature, here, is the peaking curve shapes. In Fig. (4), the multiplicity range as well as the broadening of the distributions increases with target size as well as energy. The geometrical model considering the overlap size between target and projectile seems to be effective in drawing the characteristic features of the distributions. Accordingly the effect of the target size is reflected on the impact parameter value and consequently on the energy participation, which is the main effective parameter in particle creation. The modified FRITIOF model overestimates the data associated with the H target nuclei as well as for those associated with all targets at 2.1A GeV. The model can reproduce the distributions at 3.7A GeV for all targets beyond hydrogen. Both the experimental and theoretical distributions are fitted well by the Gaussian shapes presented by the smooth solid and dashed curves, respectively. Thus, it is reasonable to say that the mechanism in this system of particle production in the FHS is completely different from that in the BHS.

Journal of. Modern Trends in Physics Research
Online ISSN 2636-4220
DOI: 10.19138/mtpr/(14)137-147
Accepted: 2014-12-19

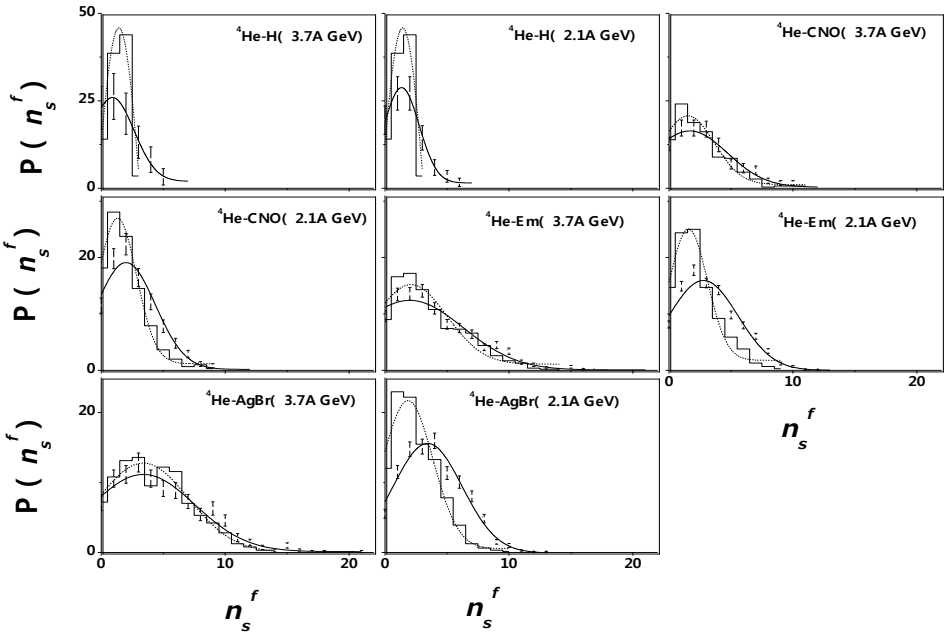

Fig. (4): The multiplicity distributions of the forward emitted shower particle in 2.1A and 3.7A GeV ^{4}He interactions with H, CNO, Em, and AgBr nuclei, together with the predictions of the modified FRITIOF model and the Gaussian fitting.

Production Probability of Pion in BHS

The percentage probability of the backward emitted shower particle production, P (n_s^b> 0) %, is defined as, the number of events having (n_s^b> 0) normalized to the total sample of events. In Fig. (5) this probability is evaluated as a function of the target mass number for the present interactions. From Fig. (5), one observes the strong dependence of backward relativistic hadron production on the target size. This strong dependence is evaluated linearly by Eq. (6) and presented in Fig. (5) by the straight lines. Independently on the projectile size (A_{Proj} = 1 to 32) or energy (E_{lab} = 2.1A to 200A GeV), the backward relativistic hadron is produced with probability values of ~ 20 to 30% for interactions with Em target[31]. The theoretical predictions of the FRITIOF model agree with the data, especially at 3.7A GeV. The fit parameters μ and ν are tabulated in Table (6).

$$P(n_s^b > 0)\% = \mu + \nu A_T \qquad (6)$$

Journal of. Modern Trends in Physics Research
Online ISSN 2636-4220
DOI: 10.19138/mtpr/(14)137-147
Accepted: 2014-12-19

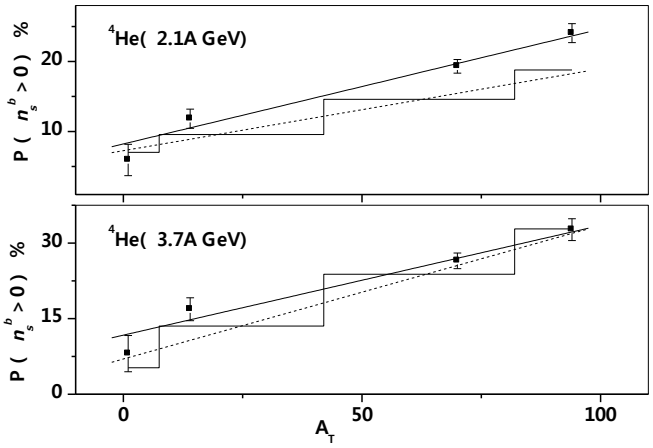

Fig. (5): The probability of the backward emitted shower particle multiplicity, in the interactions of 2.1A and 3.7A GeV ^{4}He with emulsion nuclei, as a function of the target mass number, together with the predictions of the modified FRITIOF model and the fitting lines.

Table (6): The fit parameters of Eq. (6).

E_{lab}/A GeV	μ	ν
2.1	8.22±1.42 (7.26±0.69)	0.16±0.02 (0.12±0.01)
3.7	11.72±2.22 (6.99±2.16)	0.22±0.03 (0.27±0.04)

Average Multiplicity

The average multiplicities of the forward and backward shower particles, emitted in the present interactions, are correlated with the target size in Fig. (6). the correlation reveals a linear dependence, for the backward emitted shower particle, presented by the straight lines. Eq. (7) approximates the values of fit parameters, a_s^b and b_s^b, to be listed in Table (7). The model reproduces the linear correlation especially at 3.7A GeV. The slope parameter ~ 0 and the intercept parameter ~ 0.1, irrespective of the energy.

$$<n_s^b> = a_s^b + b_s^b A_T \quad (7)$$

Journal of. Modern Trends in Physics Research
Online ISSN 2636-4220
DOI: 10.19138/mtpr/(14)137-147
Accepted: 2014-12-19

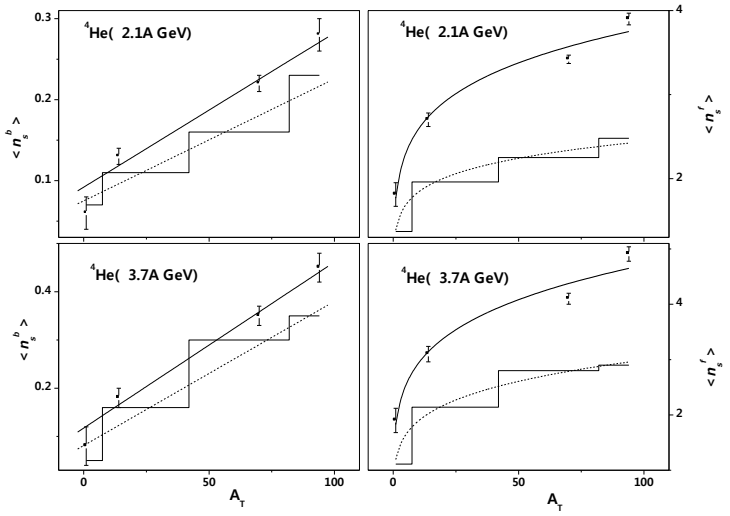

Fig. (6): The dependence correlations of the forward and backward emitted shower particle average multiplicities on the target size in the present interactions, together with the theoretical prediction.

In experiment (31), using a wide range of projectile size (A_{Proj} = 1 to 32) interacting in nuclear emulsion at Dubna energy, the values of $<n_s^b>$ are found to increase with projectile size for $A_{Proj} < 6$. At $A_{Proj} \geq 6$, they began to saturate and had a constant value of $<n_s^b> \sim 0.4$. In this experiment the results imply that the energy is not an effective parameter in backward shower emission. Therefore, one can conclude that, while the average shower particle multiplicity, emitted in the BHS, depends on the target size, it depends neither on the projectile size nor energy. This confirms our expectation that, the backward relativistic hadron does not come from the fireball nuclear matter or hadronic matter. They are target source particles, regarding the nuclear limiting fragmentationregime. In Fig. (6), the forward emitted shower particle average multiplicity shows higher values than the backward ones. It increases with the energy as well as target size. The increase with the target size, here, does not mean that this particle is a target source but the target size enhances in the total system size which affects the participant matter size. Although the dependence on the target size is strong, however it has often a tendency of saturation at $A_T > 14$. This behavior may be reflected on the dependence which is approximated well by a power law relation of Eq. (8). This approximation is presented in Fig. (6) by the smooth curves. The fit parameters, a_s^f and b_s^f, are listed in Table (7). From Fig. (6), one can observe also that the model underestimates the data. Abdelsalam et al (31) determine the dependence of $<n_s^f>$ on the projectile mass number at Dubna energy. They find that dependence as; $< n_s^f >= 1.89 A_{proj}^{0.56}$, i. e. $< n_s^f > \propto r_{proj}^{2/3}$.

$$< n_s^f > = a_s^f A_T^{b_s^f} \quad (8)$$

Comparing this dependence by Eq. (8), it can be observed that the majority contribution of the participant matter is accounted from the projectile throughout the production of the forward emitted shower particle. Thus, while the production source of the backward emitted shower particle is the target fragmentation system the forward emitted one is originated mainly from a creation system provided by the participant energy.

Table (7): The fit parameters of Eq. (7) and Eq. (8).

E_{lab}/A GeV	a_s^b	b_s^b	a_s^f	b_s^f
2.1	0.092±0.016 (0.075±0.016)	0.002±0 (0.002±0)	1.77±0.13 (1.39±0.07)	0.17±0.02 (0.12±0.01)
3.7	0.117±0.020 (0.081±0.029)	0.003±0 (0.003±0)	1.83±0.23 (1.20±0.09)	0.21±0.03 (0.20±0.02)

Journal of. Modern Trends in Physics Research
Online ISSN 2636-4220
DOI: 10.19138/mtpr/(14)137-147
Accepted: 2014-12-19

CONCLUSIONS

From the analysis of 2.1A and 3.7A GeV α–particle interactions, using photographic nuclear emulsion detector, we conclude the following:

1- The inelastic interaction cross section of α–particle in nuclear emulsion is approximated as a function of the target mass number. In the present energy region, the cross section is independent on the energy. It can be determined in the light of the Glauber's multiple scattering theory.Therefore, the interaction cross–sectional values can be obtainable when planning and equipping for a therapy program in which the relativistic α–particle is used.

2- The dominant mechanism characterizing the backward shower particle production is the decay behavior. There is no energy effect on the backward production. The multiplicity distribution of this hadron is expressed in terms of the target size. While the production probability of this hadron is independent on the projectile size or energy it increases linearly with the target size. While the average backward shower particle multiplicity tends to a limited value ~ 0.4, irrespective of the projectile size or energy, it increases linearly with the target size. Hence, the main effective parameter is the target size, regarding the nuclear limiting fragmentation beyond 1A GeV. Thus, such hadron is expected to be decayed through the de–excitation of the excited target nucleus as similar as the compound nucleus mechanism.

3- In the FHS the shower particle multiplicity distributions are peaking shaped, where they can be described well by the Gaussian shapes. The production of the forward emitted relativistic hadron is attributed to a mechanism, which is completely different from that in BHS. Although the target nucleus is not the source of the forward relativistic hadron, however the target size is an effective parameter in this production as well as the projectile size. The geometrical concept underlying the nuclear fireball model may interpret the effect of the projectile and target sizes in particle production at high energy. The effect of the target size on the forward shower particle production is reflected on their multiplicity characteristics at each target. Regarding the incident energy role as a principal parameter affecting the forward relativistic hadron production, this system of production is regarded as a particle creation system, in which the particles are sourced from hadronic matter or fireball nuclear matter.

4- The modified FRITIOF model can predict the system of the relativistic hadron production in the BHS well. In the FHS the hadronization system can be described satisfactorily. This suggests that the Reggeon picture can be considered as a plausible development to the Model. Sometimes underestimations or overestimations are observed in the model predictions with experimental data. This may require a modern approach in describing nuclear cascading.

5- For the pion, as a final state hadron, the backward emits shower particle is associated with the target fragmentation. Accordingly, its production is easily available beyond the nuclear limiting fragmentation onset (~ 1A GeV). Therefore, this hadron can be more obtainable practically as a source of therapy requirements.

ACKNOWLEDGEMENT

We owe much to Vekseler and Baldin High Energy Laboratory, JINR, Dubna, Russia, for supplying us the photographic emulsion plates irradiated at Synchrophasotron.

REFERENCES

(1)J. P. Bondorf, A. S. Botvina, A. S. Iljinov, I. N. Mishustin, and K. Sneppen; Phys. Rep. 257; 133 (1995).
(2) J. P. Bondorf; Journal de Physique 37/C5; 195 (1976); Proceeding of the EPS topical conference on Large Amplitude Collective Nuclear Motions, Keszthely; Hungary; June 1979.
(3)J. Miller; 1st International Workshop on Space Radiation Research and 11th Annual NASA Space Radiation Health Investigators; Workshop Arona (Italy); May 27–31, 2000; Physica Medica–Vol. XVII; Supplement 1; 2001.
(4) I. Schall, D. Schardt, H. Geissel, H. Irnich, E. Kankeleit, G. Kraft, A. Magel, M. Mohar, G. Münzenberg, F. Nickel, C. Scheidenberger, W. Schwab; Nucl. Instr. and Meth. B 117; 221 (1996).
(5) I. Schall, D. Schardt, H. Geissel, H. Irnich, E. Kankeleit, G. Kraft, A. Magel, M. Mohar, G. Münzenberg, F. Nickel, C. Scheidenberger, W. Schwab, L. Sihver; Adv. Space Res. B 17; 87 (1996).

Journal of. Modern Trends in Physics Research
Online ISSN 2636-4220
DOI: 10.19138/mtpr/(14)137-147
Accepted: 2014-12-19

(6) C. Von Essen, M. Bagshaw, S. Bush, A. Smith, M. Kligerman; "Long–Term Results of Pion Therapy at Los Alamos" (September 1987); Int. J. Radiat. Oncol. Biol. Phys. 13; 1389 (1987).
(7) George B. Goodman; for TRIUMF Cancer Therapy with Pions; Proceedings of the 13th International Conference on Cyclotrons and their Applications; Vancouver BC; Canada; 6 – 10 July; 242 (1992).
(8) Petti and Lennox; Ann. Rev. Nuclear & Particle Science 44; 154 (1994).
(9) http://www.klinikum.uni-heidelberg.de/index.php?id=113005&L=1
(10) CERN COURIER Nov 23; 2011.
(11) J. Benecke, T. T. Chou, C. N. Yang, and E. Yen; Phys. Rev. 188; 2159 (1969).
(12) Fu–Hu Liu; Chinese Journal of Physics 40; 159 (2002).
(13) M. S. Ahmad, M. Q. R. Khan, and R. Hasan; Nucl. Phys. A 499; 821 (1989).
(14) W. R. Webber; Proceedings of the international Cosmic Ray Conference; Vol. 8; P. 65; Moscow; USSR (1987).
(15) P. L. lindstorm, D. E. Greiner, H. H. Heckman, and B. Cork; Lawrence Berkeley Laboratory Report; LBL–3650; 1975.
(16) D. L. Olson, B. L. Berman, D. E. Grenier, H. H. Heckman, P. J. Lindstrom, and H. J. Crawford; Phys. Rev. C 28; 1602 (1983).
(17) M. S. El–Nagdy, A. Abdelsalam, Z. Abou–Moussa, and B. M. Badawy; Can. J. Phys. 91; 737 (2013).
(18) A. Abdelsalam, N. Metwalli, S. Kamel, M. Aboullela, B. M. Badawy, and N. Abdallah; Can. J. Phys. 91; 438 (2013).
(19) A. Abdelsalam, B. M. Badawy, and M. Hafiz; J. Phys. G: Nucl. Part. Phys. 39; 105104 (2012).
(20) C. F. Powell, F. H. Fowler, and D. H. Perkins; The Study of Elementary Particles by the Photographic Method; Pergamon Press. London; New York; Paris; Los Angles; 474 (1958).
(21) H. Barkas; Nuclear Research Emulsion; Vol. I; Technique and Theory Academic Press Inc.; (1963).
(22) S. Yu. Shmakov and V. V. Uzhinskii; Com. Phys. Comm. 54; 125 (1989).
(23) J. R. Florian et al; Report Submitted to the Meeting of Division of Particles and Fields; Berkeley; California; 1973.
(24) A. Abdelsalam; JINR Report (Dubna); E1–81–623 (1981).
(25) E. O. Abdrahmanov et al; Z. Phys. C 5; 1 (1980).
(26) M. I. Adamovich et al (EMU01 Collaboration); Lund University Report; Sweden; LUIP 8904; May (1989).
(27) B. Andersson, G. Gustafson, and B. Nilsson–Almqvist; Nucl. Phys. B 281; 289 (1987).
(28) B. Nilsson–Almqvist, E. Stenlund; Comp. Phys. Comm. 43; 387 (1987).
(29) A. Abdelsalam, E. A. Shaat, N. Ali–Mossa, Z. Abou–Mousa, O. M. Osman, N. Rashed, W. Osman, B. M. Badawy, and E. El–Falaky; J. Phys. G : Nucl. Part. Phys. 28; 1375 (2002).
(30) A. Abdelsalam, B. M. Badawy, and E. El–Falaky; Can. J. Phys. 85; 837 (2007).
(31) A. Abdelsalam, M. S. El–Nagdy, and B. M. Badawy; Can. J. Phys. 89; 261 (2011).